Supplementary Information

Ideal PN Photodiode using Doping Controlled WSe_2-$MoSe_2$ Lateral Heterostructure

Ji Eun Kim[a], Won Tae Kang[a,b], Van Tu Vu[a], Young Rae Kim[a,b], Yong Seon Shin[a], Ilmin Lee[a], Ui Yeon Won[a], Boo Heung Lee[a], Kunnyun Kim[c], Thanh Luan Phan[a*], Young Hee Lee[b,d], and Woo Jong Yu[a*]

1. Role of NaOH as the promoter

We chose NaOH as a promoter. It has been reported that the promoter plays important role in enhancing the growth because it can create more vapor of growth precursor as well as decrease the melting point.[1] The $MoSe_2$ can be fast grown at low temperature without the NaOH assistant due to the presence of Na as the promoter, as seen in the previous report.[2] After CVD grown $MoSe_2$ was finished, then Nb-doped WSe_2 started growing along the edge of as-grown $MoSe_2$ due to rich defects. However, Nb-doped WSe_2 has only formed particles due to low chemical activity and a high melting point of WO_3 without the assistance of NaOH promoter, as demonstrated in Figure S1. The existence of Na from AMT is insufficient for the enhanced growth of Nb-doped WSe_2 The W and Nb oxide species will react with NaOH to create the active $Na_2W_xNb_{1-x}O_4$ compound. The possible reaction route of $MoSe_2$ and Nb-doped WSe_2 during growth are as follow.

$$Na_2MoO_4 + 2H_2 + Se = MoSe_2 + 2H_2O + Na_2O$$

$$Na_2W_xNb_{1-x}O_4 + Se + H_2 = 2W_xNb_{1-x}Se_2 + Na_2SeO_3 + H_2O$$

Beside NaOH, other alkali metal promoter such as NaCl, KCl, KOH etc can be used as effective promoters as demonstrated in the previous report.[3]

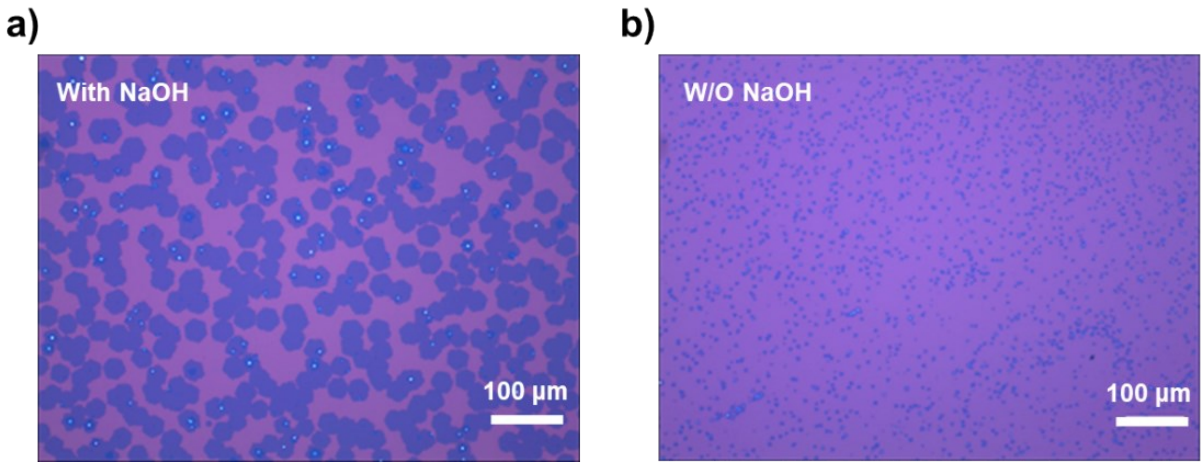

Figure S1. Effect of NaOH promoter on Nb-doped WSe_2 via CVD growth.

2. Ideality factor of the PN diode

The ideality factor of the PN diode can be extracted from the slope of the ln I–V equation of

$$J = J_0(e^{qV_a/nKT} - 1) \quad (1)$$

where n is the diode quality factor, which ranges from 1 to 2, q is the electric charge $1.6E^{-19}$ (C), k_B is the Boltzmann constant $1.37E^{-23}$(J/K), and T is the absolute temperature of 273.14 K. In the $\ln(J) - V$ relational expression ($\ln(J) = \ln(J_0) + q/nKT \times V_a$), the n term can be obtained by assigning the constant values of q, kB, and T to the slope. Thus, with the measured data, n is calculated to be 1.3, which is close to the ideality factor of 1 (inset graph of Figure 3h).

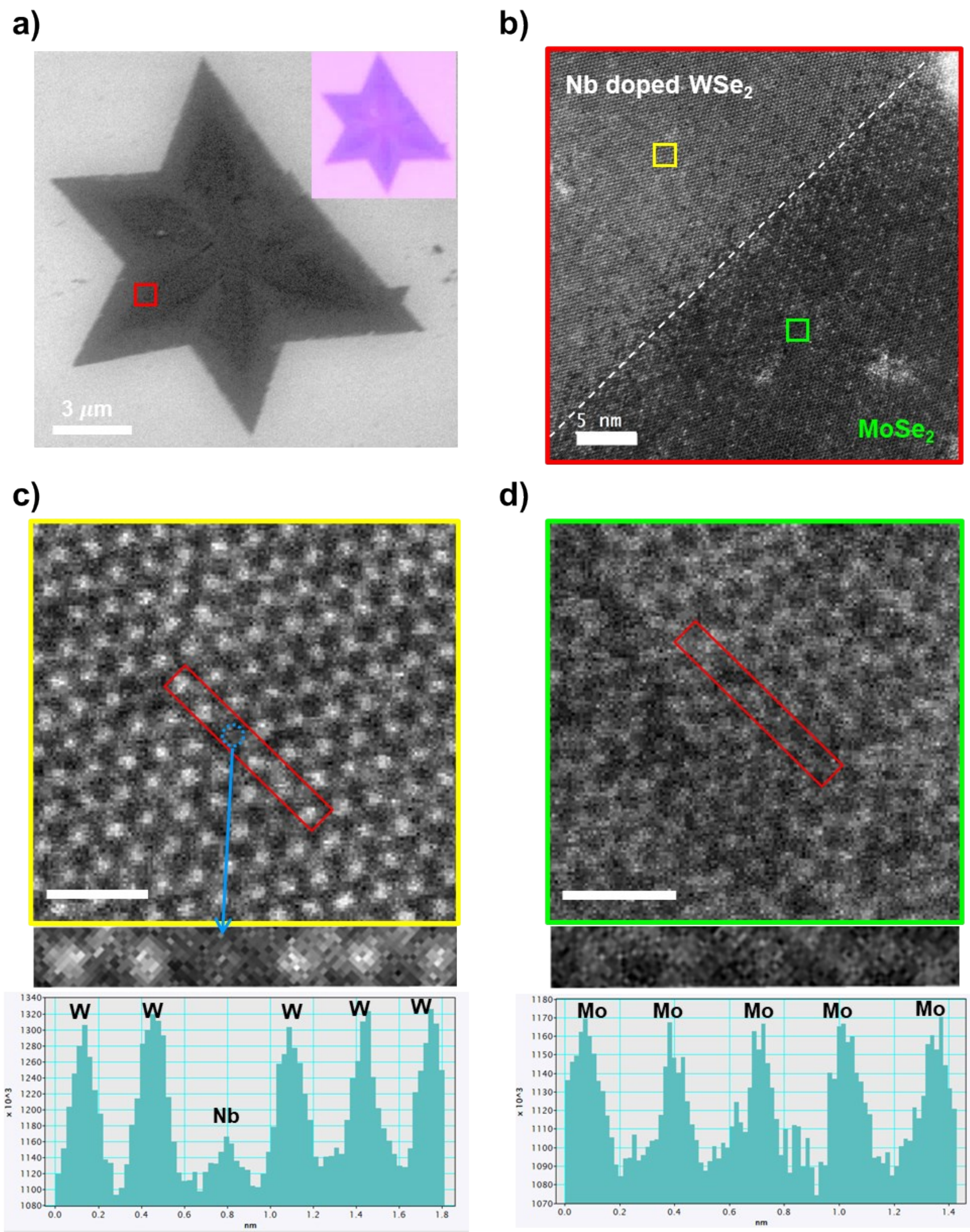

Figure S2. FESEM (a) and STEM (b-d) image of the CVD-grown Nb-doped WSe_2-$MoSe_2$ lateral heterostructure. The scale bars of c) and d) indicate 0.7 nm.

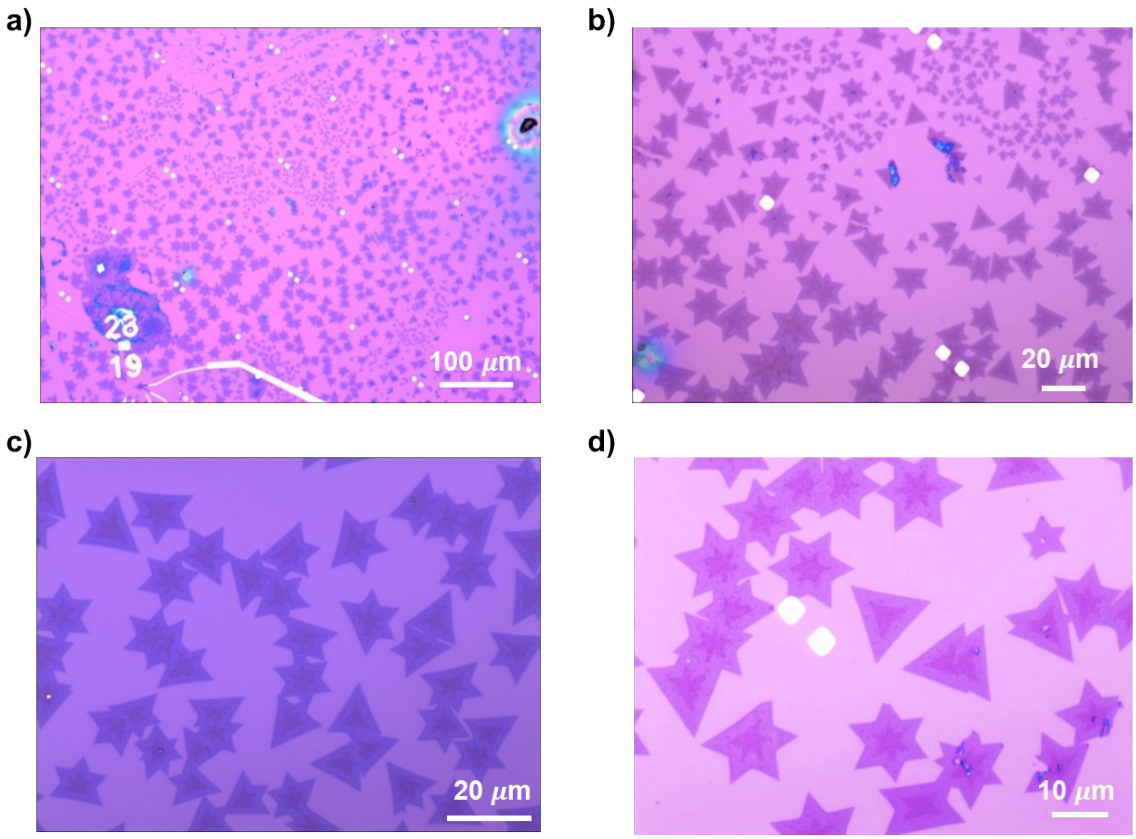

Figure S3. High yield of the CVD-grown Nb-doped WSe_2-$MoSe_2$ lateral heterostructure.

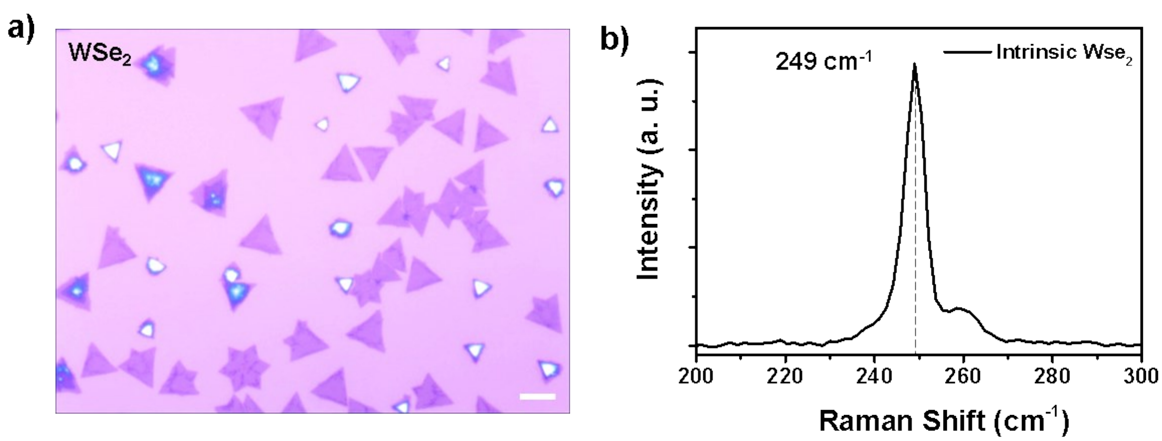

Figure S4. a) Optical microscopic image of the CVD-grown intrinsic WSe_2. The scale bar is 10 μm b) Raman spectrum of the WSe_2. The main peak is 249 cm^{-1}.

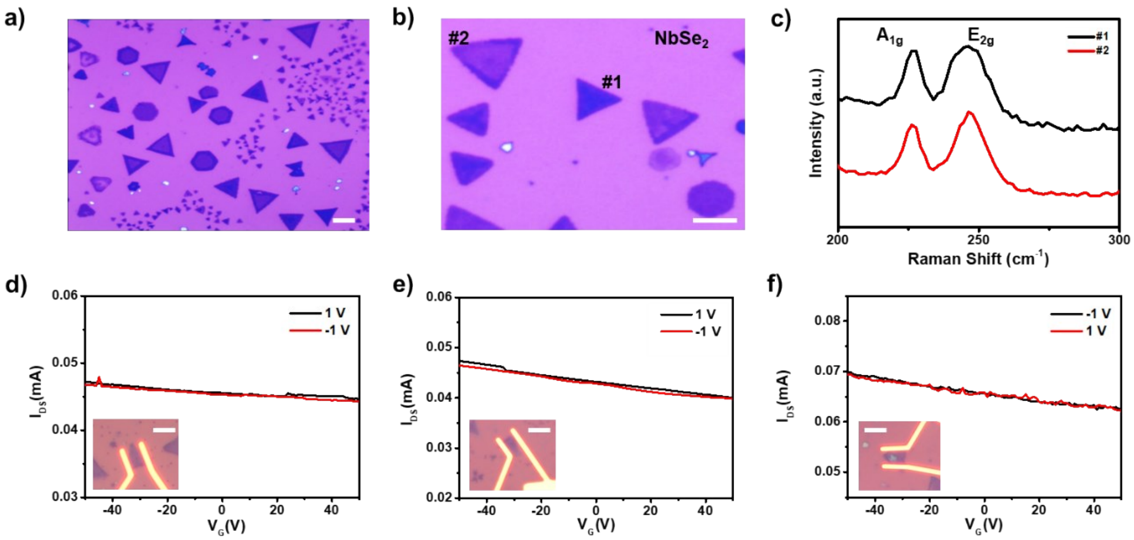

Figure S5. a) Optical microscopic image of the CVD-grown $NbSe_2$. All scale bars are 10 μm. b) Expanded image. c) Raman spectra from sample #1, #2 of b. d–f) Metallic properties of the CVD-grown $NbSe_2$.

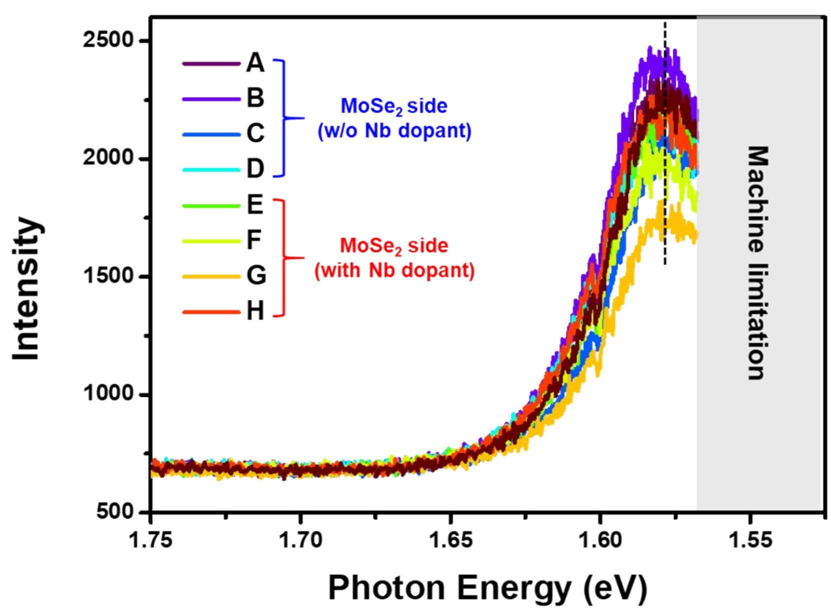

Figure S6. PL spectrum of $MoSe_2$ domain in WSe_2-$MoSe_2$ heterostructure with and without Nb-dopant

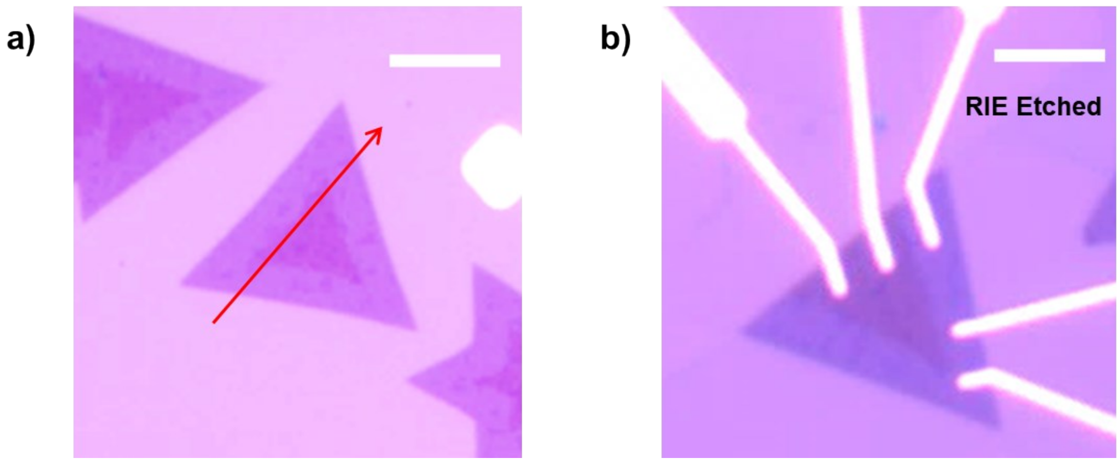

Figure S7. a) Optical microscopic image of the CVD-grown lateral heterostructure. b) Etched flakes by RIE using SF_6. All scale bars are 5 μm.

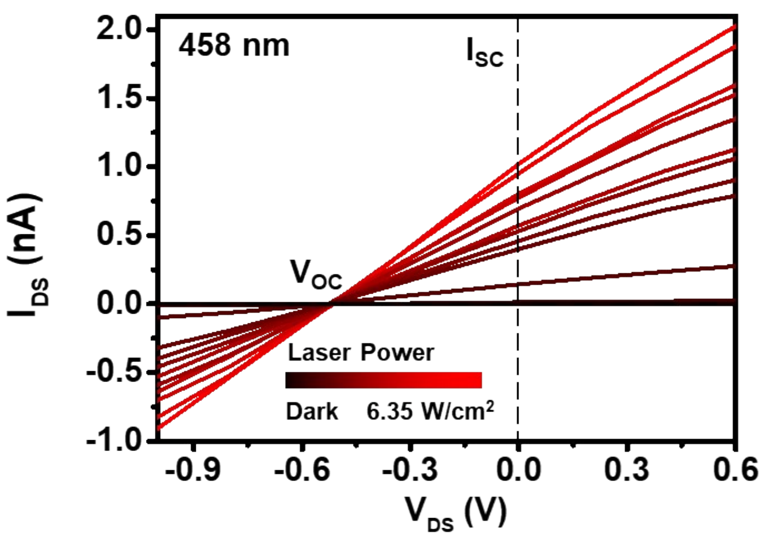

Figure S8. Short-circuit current and open-circuit voltage under 458 nm laser. The open-circuit voltage is about 0.52 V.

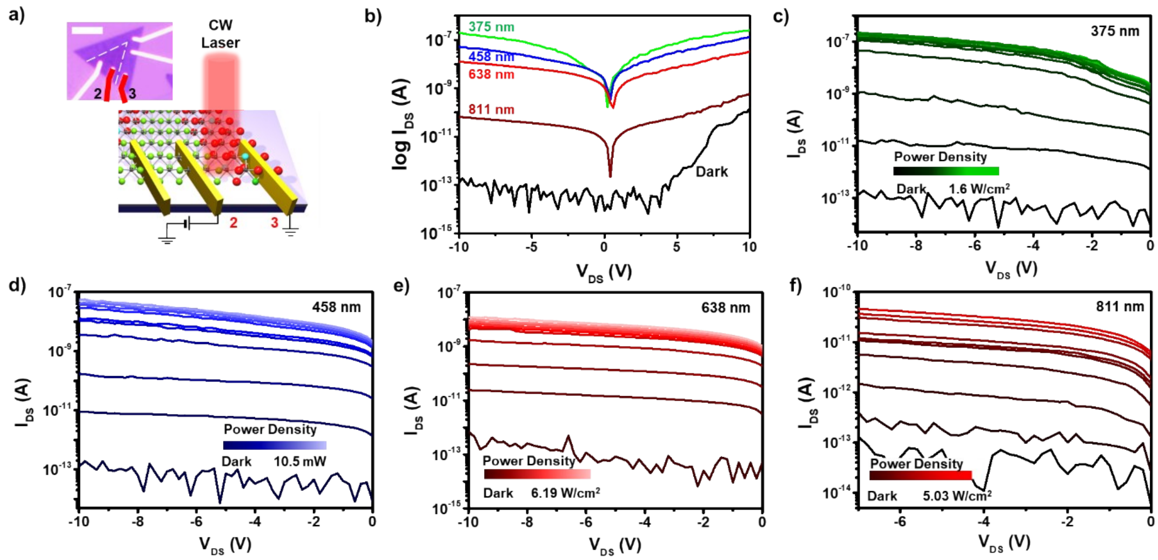

Figure S9. Photocurrent under different laser powers with various wavelengths such as a) 375 nm, b) 458 nm, c) 638 nm, d) 811 nm. The scale bar in the inset image of a) is 5μm

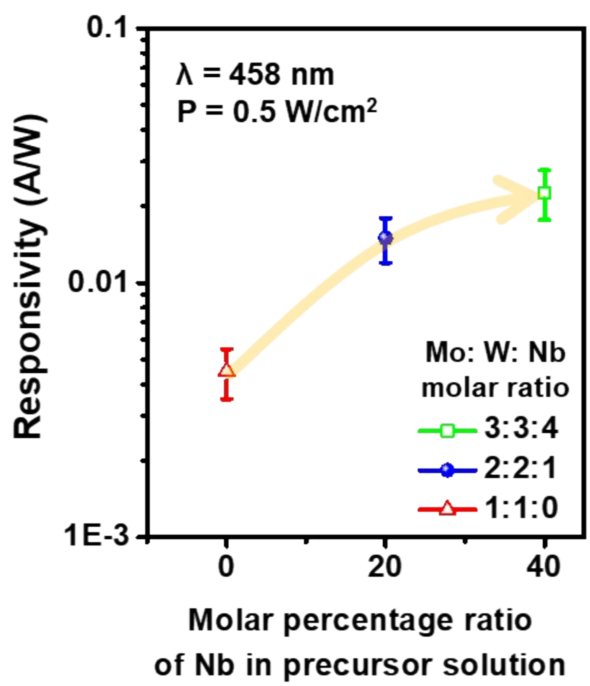

Figure S10. The photoresponsivity and Nb dopant dependence in WSe_2-$MoSe_2$ lateral heterostructure.

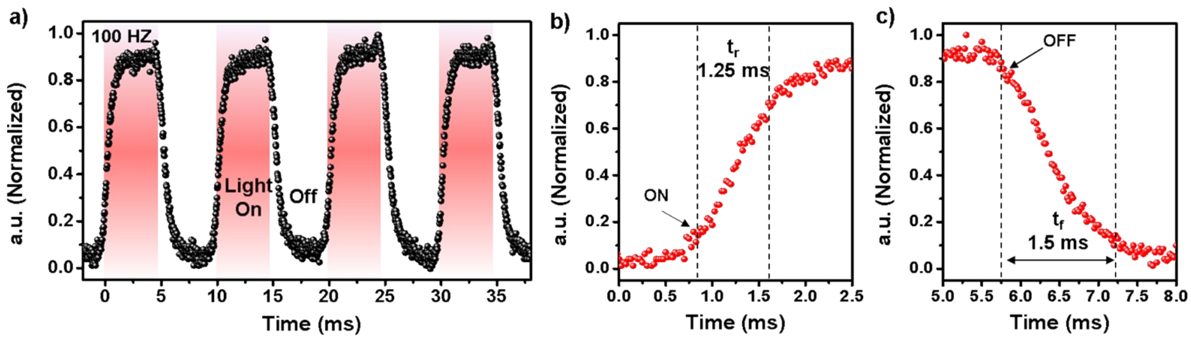

Figure S11. a) Photocurrent response, the laser light is turned on/off by a mechanical chopper worked at 100 Hz under illuminating 375 nm laser. b–c) The graph magnifies the rising and falling portion of the photocurrent. Rise and fall times are on the millisecond time scale.

Table S1. Performance comparison tables with other 2D photodetectors

Device structure	Material	Synthetic method	Measure Condition	I_{Light}/I_{Dark} Max	R [A · W^{-1}] Max	D* [*Jones*] Max	t_r, t_f [ms]	ref
Lateral p-n	Nb-doped WSe_2-$MoSe_2$	CVD	357 ~ 811 nm V_d = 0 V V_g = 0 V	>10^5	0.33	5.78 × 10^{15}	1.25, 1.5	Our
	WSe_2-$MoSe_2$	CVD	543 nm V_d = 0	10^2	-	-	6	[4]
	MoS_2-WS_2	CVD	532 nm V_d = 0 V V_g = 0 V	10^3	4.36×10^{-3}	4.36 × 10^{13}	4	[5]
	WS_2-WSe_2	CVD	514 nm V_d = 0 V V_g = 0 V	< 10^1	44 ×10^{-3}	-	0.1	[6]
	Bilayer (2L) MoS_2-WS_2	CVD	457 ~ 671 nm V_d = 5 V V_g = 0 V	10^3	6.72 × 10^3	3.09 × 10^{13}	39, 47	[7]
	1L-2L Wse_2	CVD	532 nm V_d = 2 V V_g = -80 V	10^1	109.75	5.4 × 10^{11}	290, 250	[8]
	Partially	Exfoliation	1550 nm V_d = 5 V	< 10^1	6.2 ×10^{-3}	1.04 × 10^{11}	3, 10	[9]

	Doped-Bp		$V_g = -10$ V					
	Partially Doped-Wse_2	Exfoliation	365~740 nm	10^2	30×10^{-3}	6.18×10^8		[10]
	Partially Doped-Wse_2	Exfoliation	500 nm $V_d = 1$ V $V_g = 0$ V	$< 10^1$	5.07	3×10^{10}	100, -200	[11]
	MoS_2-WS_2	CVD	514 nm	-	-	-	-	[12]
	Multilayer MoS_2-WS_2	Exfoliation	633 nm	10^2	0.76			[13]
Vertical p-n	WSe_2-$MoSe_2$	CVD	$V_d = 0.1$ V $V_g = 0$ V	10^1	-	-	-	[14]
	MoS_2-WSe_2	CVD	532 nm $V_d = 0$ V V_g = 0 V	-	0.002	-	0.1	[15]
	2L-2L MoS_2-WSe_2	CVD	532 nm $V_d = 0$ V $V_g = 0$ V	-	-	-	-	[16]
	ML-ML MoS_2-WS_2	Exfoliation	633 nm	10^1	1.42	-	-	[13]
Single TMD	$MoSe_2$	CVD	650 nm	10^2	-	-	-	[17]
	$MoSe_2$	CVD	532 nm $V_d = 10$ V $V_g = 0$ V	10^2	0.013	-	60	[18]

Table S2. Performance comparison tables with other 2D photodetectors

Device structure	Material	Thickness	Rectification Ratio	V_{OC}	ref
Lateral p-n	Nb-doped WSe_2-$MoSe_2$	1L	10000	0.52 V	our
	WS_2 -MoS_2	1L	100	0.12 V	[6]
	WSe_2-WS_2	ML	-	0.47 V	[6]
	In_2Se_3-$CuInSe_2$	14	10	0.03 V	[9]
	WS_2-MoS_2	2L	1000	-	[7]
	WSe_2-MoS_2	1L	10	0.22 V	[20]

MoS_2-WS_2	1L	-	0.32 V	[5]

References

1 1 Q. Feng, M. Zhu, Y. Zhao, H. Liu, M. Li, J. Zheng, H. Xu and Y. Jiang, *Nanotechnology*, 2018, **30**, 34001.

2 S. Boandoh, S. H. Choi, J. H. Park, S. Y. Park, S. Bang, M. S. Jeong, J. S. Lee, H. J. Kim, W. Yang, J. Y. Choi, S. M. Kim and K. K. Kim, *Small*, 2017, **13**, 1–9.

3 H. Kim, G. H. Han, S. J. Yun, J. Zhao, D. H. Keum, H. Y. Jeong, T. H. Ly, Y. Jin, J. H. Park, B. H. Moon, S. W. Kim and Y. H. Lee, *Nanotechnology*, , DOI:10.1088/1361-6528/aa7e5e.

4 S. Jia, Z. Jin, J. Zhang, J. Yuan, W. Chen, W. Feng, P. Hu, P. M. Ajayan and J. Lou, *Small*, 2020, **2002263**, 1–7.

5 W. Wu, Q. Zhang, X. Zhou, L. Li, J. Su, F. Wang and T. Zhai, *Nano Energy*, 2018, **51**, 45–53.

6 X. Duan, C. Wang, J. C. Shaw, R. Cheng, Y. Chen, H. Li, X. Wu, Y. Tang, Q. Zhang, A. Pan, J. Jiang, R. Yu, Y. Huang and X. Duan, *Nat. Nanotechnol.*, 2014, **9**, 1024–1030.

7 K. Ye, L. Liu, Y. Liu, A. Nie, K. Zhai, J. Xiang, B. Wang, F. Wen, C. Mu, Z. Zhao, Y. Gong, Z. Liu and Y. Tian, *Adv. Opt. Mater.*, 2019, **7**, 1–7.

8 R. Cheng, D. Li, H. Zhou, C. Wang, A. Yin, S. Jiang, Y. Liu, Y. Chen, Y. Huang and X. Duan, *Nano Lett.*, 2014, **14**, 5590–5597.

9 Y. Liu, Y. Cai, G. Zhang, Y. W. Zhang and K. W. Ang, *Adv. Funct. Mater.*, 2017, **27**, 1–9.

10 M. Sun, D. Xie, Y. Sun, W. Li, T. Ren, *Nanotechnology* **2018**, *29*, 015203.

11 Z. Q. Xu, Y. Zhang, Z. Wang, Y. Shen, W. Huang, X. Xia, W. Yu, Y. Xue, L. Sun, C. Zheng, Y. Lu, L. Liao, Q. Bao, *2D Mater.* **2016**, *3*, 041001.

12 K. Chen, X. Wan, J. Wen, W. Xie, Z. Kang, X. Zeng, H. Chen, J. Bin Xu, *ACS Nano* **2015**, *9*, 9868.

13 N. Huo, J. Kang, Z. Wei, S. S. Li, J. Li, S. H. Wei, *Adv. Funct. Mater.* **2014**, *24*, 7025.

14 Y. Gong, S. Lei, G. Ye, B. Li, Y. He, K. Keyshar, X. Zhang, Q. Wang, J. Lou, Z. Liu, R. Vajtai, W. Zhou and P. M. Ajayan, *Nano Lett.*, 2015, **15**, 6135–6141.

15 C. H. Lee, G. H. Lee, A. M. Van Der Zande, W. Chen, Y. Li, M. Han, X. Cui, G. Arefe, C. Nuckolls, T. F. Heinz, J. Guo, J. Hone and P. Kim, *Nat. Nanotechnol.*, 2014, **9**, 676–681.

16 Y. Gong, J. Lin, X. Wang, G. Shi, S. Lei, Z. Lin, X. Zou, G. Ye, R. Vajtai, B. I. Yakobson, H. Terrones, M. Terrones, B. K. Tay, J. Lou, S. T. Pantelides, Z. Liu, W. Zhou, P. M. Ajayan, *Nat. Mater.* **2014**, *13*, 1135.

17 Y.-H. Chang, W. Zhang, Y. Zhu, Y. Han, J. Pu, J.-K. Chang, W.-T. Hsu, J.-K. Huang, C.-L. Hsu, M.-H. Chiu, T. Takenobu, H. Li, C.-I. Wu, W.-H. Chang, L.-J. L. Andrew Thye Shen Wee, *ACS Nano* **2019**, *8*, 8582.

18 J. Xia, X. Huang, L. Z. Liu, M. Wang, L. Wang, B. Huang, D. D. Zhu, J. J. Li, C. Z. Gu, X. M. Meng, *Nanoscale* **2014**, *6*, 8949.

19 Z. Zheng, J. Yao, G. Yang, *ACS Appl. Mater. Interfaces* **2017**, *9*, 7288.

20 M. Y. Li, Y. Shi, C. C. Cheng, L. S. Lu, Y. C. Lin, H. L. Tang, M. L. Tsai, C. W. Chu, K. H. Wei, J. H. He, W. H. Chang, K. Suenaga, L. J. Li, *Science (80-.).* **2015**, *349*, 524.